Kent Academic Repository

Downloaded from

The version of record is available from

This document version

Author's Accepted Manuscript

DOI for this version

Licence for this version

UNSPECIFIED

Additional information

Versions of research works

Homogeneity of Modifier Ion Distributions and the Mixed Alkaline Earth Effect (MAEE) in MgO-CaO-SiO$_2$ Silicate Glasses using Molecular Dynamics

Laura A. Swansbury and Gavin Mountjoy*

School of Physical Sciences, University of Kent, Canterbury, Kent, CT2 7NH, U.K.

Abstract

Oxide glasses containing a mixture of modifier ions have a wide range of applications, and it is often assumed that these modifier ions mix homogenously in the melt. Silicate glasses are known for their significant industrial importance and are often doped with magnesium and calcium modifier ions to utilise their properties for applications. This study investigated the structural and dynamical impact imposed on a glass by the presence of two different types of alkaline earth cations. This was achieved through increasingly substituting magnesium for calcium in xMgO-(50-x)CaO-50SiO$_2$ glasses which were modelled computationally using classical molecular dynamics simulation (MD). A mixed alkaline earth effect (MAEE) was found to cause the suppression of the modifier ion diffusivity. An absence of any significant deviation from the expected trends in the structural investigations confirmed that the MAEE is not a structural effect. This MAEE was therefore analogous to the mixed alkali effect (MAE), and was most prominent for roughly equimolar mixtures of calcium and magnesium ions. Interestingly, there was also evidence of the diffusivity being enhanced when only a small amount of a second alkaline earth ion was added.

Introduction

Among the classification of glasses, oxide glasses have received the most attention in terms of research and applications. The strongly established modified random network model [1] recognises the role of special p-block elements (Si, B, P, and Ge) as glass formers which are required to obtain a glass network. Foremost among these, and coinciding with the natural abundance of silicon and oxygen ions, are silicate glasses. In contrast, s-block elements of alkali and alkaline earth ions are network modifiers, and disrupt the connectivity of the glass network. Although the latter may seem detrimental, it is essential for achieving economic production of glasses for applications. The role of modifier ions has been thoroughly investigated for both fundamental glass science and for applications. A contemporary example the latter is the diffusion of alkali ions, where Li ion conductivity is central to Li ion battery technology. The modified random network model predicts that modifier ions occupy "channels", hence understanding the diffusion of alkali ions is linked to understanding of the glass structure.

Among the key phenomena observed in alkali silicate glasses is the mixed alkali effect (MAE) [2]. Glasses containing a mixture of two alkali ion types have suppressed conductivity relative to the endpoint compositions which only contain one alkali ion type. Figure 1 (left) illustrates this effect for

electrical conductivity measurements on $(K_xNa_{1-x})_2Si_4O_9$ glasses [3]. The MAE is smallest for alkali ions of a similar size, and is larger for alkali ions of notably different size. Studies indicate that the coordination numbers of alkali ions is not significantly different in a mixed alkali glass compared to the endpoint compositions. Instead, the distribution of neighbouring alkali ions is expected to follow trends based on random mixing. A possible way to link the local atomic environment (structure) and diffusion (dynamics) of modifier ions is to consider that in a mixed alkali silicate glass, diffusion may be hindered if there are two different sizes of modifier ion sites which are not interchangeable.
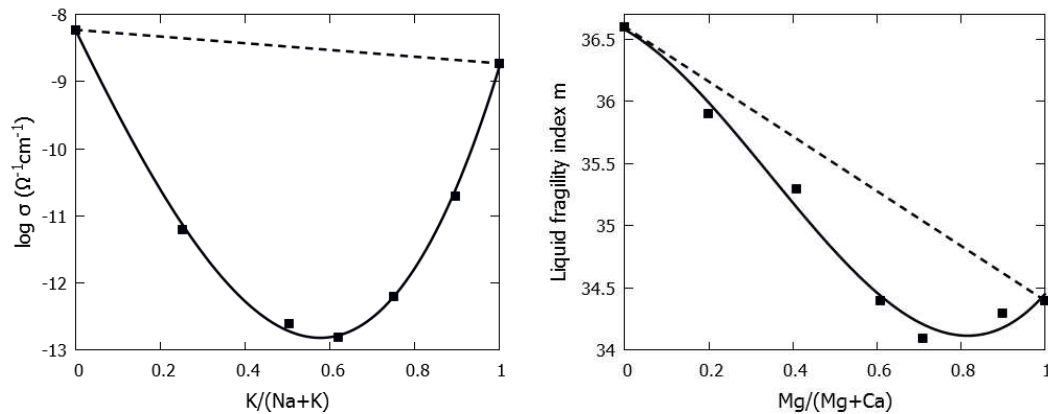

Figure 1: To the left, electrical conductivity measurements on $(K_xNa_{1-x})_2Si_4O_9$ glasses [3]. To the right, liquid fragility index values for sodium aluminosilicate glasses [4]. (In each case the dashed line shows a linear trend between endpoint compositions, and the solid line is a cubic fit to the data.)

Recently, a handful of studies have proposed that a mixed alkaline earth effect (MAEE) occurs in oxide glasses when one alkaline earth ion is substituted for another [4]. The MAEE is known to affect ion motion, and ultimately cause deviation from linearity in the dynamic properties of the glass. Figure 1 (right) illustrates this effect on the liquid fragility index of sodium aluminosilicate glasses [4]. Although the MAEE is poorly understood, it is thought to be analogous to the mixed alkali effect (MAE) which involves substituting one alkali ion for another. Studies of the MAE have been more numerous, with several different proposals on the origin of the MAE (e.g. [5], [6]). Despite this, it has been reported that the conclusions drawn about the MAE fail to satisfy all experimental findings [7]. In comparison, the MAEE has received relatively little attention, despite the need to understand ionic transport in silicate glasses containing alkaline earths [8].

Silicate glasses are ubiquitous and are well known for their industrial importance. The addition of alkaline earth modifier ions facilitates their array of applications, from construction and communications to medical implants. Modifier ions commonly include magnesium and calcium, which are the most commonly occurring alkaline earth ions in the earth's crust. Calcium is commonly featured in silicates [2] to provide durability after the addition of sodium which acts to lower the melting temperature. A silicate network disrupted by the two alkaline earth modifier ions magnesium and calcium therefore became the focus of this study.

Glasses of the metasilicate composition $xMgO-(50-x)CaO-50SiO_2$ were modelled computationally using classical molecular dynamics simulation (MD) to investigate the impact of mixing alkaline earth ions on an atomic level. To the author's knowledge, this is the first classical molecular dynamics study of the MAEE. Computational simulation was used to help comprehend why the MAEE occurs by noting when it is observed, and to what extent the amount of substituting ion affects the scale of

the MAEE. This was achieved through studying the structural and dynamical properties over the range of glass compositions.

Methodology

Interatomic potential parameters of Buckingham form were used to describe the interactions between atoms in the MgO-CaO-SiO$_2$ system. The Buckingham form is presented in equation 1 where the potential, $V_{ij}(r)$, acts between the atoms i and j which are separated by a distance r. The term q is the ion charge, and the terms A, ρ, and C are potential parameters. The interatomic potential parameters used in this work were developed by Teter [9], and are listed in table 1.

$$V_{ij}(r) = \frac{q_i q_j}{4\pi\epsilon_0 r_{ij}} + A_{ij}\exp\left(\frac{-r_{ij}}{\rho}\right) - \frac{C_{ij}}{r_{ij}^6} \qquad (1)$$

Table 1: Two-body Buckingham interatomic potential parameters from Teter [9].

i − j	q_i (e)	A (eV)	ρ (Å)	C (eV Å^6)
Si − O	2.4	13703	0.1938	54.68
Ca − O	1.2	7747	0.2526	93.11
Mg − O	1.2	7063	0.2109	19.21
O − O	-1.2	1845	0.3436	192.58

The interatomic potential parameters in table 1 were tested using the General Utility Lattice Program (GULP) [10]. This initially involved the energy minimisation of known crystalline structures using the interatomic potential parameters. The input crystalline structures used were acquired from the Crystal Structure Database (CDS) [11], and included CaO [12], MgO [13], SiO$_2$ [14], CaSiO$_3$ [15], MgSiO$_3$ [16] and MgCaSi$_2$O$_6$ [17] crystalline structures. The output structures attained following GULP energy minimisation were then compared to the input crystalline structures, and the differences between them used to assess the performance of the interatomic potential parameters. As shown in table 2, the input the output structural parameters were in close agreement, confirming the suitability of the interatomic potential parameters from Teter [9] in this study.

Table 2: Crystal lattice parameters, nearest neighbour distances (R), and coordination numbers (N(r)) for CaO, MgO, SiO_2, $CaSiO_3$, $MgSiO_3$, and $MgCaSi_2O_6$ structures before (plain text) and after (italic text) GULP energy minimisation.

Structural Parameter	CaO	MgO	SiO_2	$CaSiO_3$	$MgSiO_3$	$MgCaSi_2O_6$
Vol ($Å^3$)	28.27	19.38	113.12	795.09	832.53	226.66
	27.18	*18.24*	*114.96*	*785.95*	*854.93*	*219.75*
a (Å)	3.42	3.02	4.92	15.42	18.23	6.74
	3.38	*2.96*	*4.94*	*15.19*	*18.38*	*6.62*
b (Å)	3.42	3.02	4.92	7.32	8.82	6.74
	3.38	*2.96*	*4.94*	*7.31*	*8.87*	*6.62*
c (Å)	3.42	3.02	5.41	7.06	5.18	5.29
	3.38	*2.96*	*5.45*	*7.08*	*5.25*	*5.23*
R_{SiO} (Å)			1.61	1.62	1.64	1.63
			1.59	*1.59*	*1.59*	*1.59*
R_{CaO} (Å)	2.42			2.40		2.16
	2.39			*2.42*		2.38
R_{MgO} (Å)		2.13			2.11	2.16
		2.09			*2.13*	2.12
Si-O N(r)			4.00	4.00	4.00	4.00
			4.00	*4.00*	*4.00*	*4.00*
Ca-O N(r)	6.00			6.00		4.00
	6.00			*6.00*		*4.00*
Mg-O N(r)		6.00			6.00	6.00
		6.00			*6.00*	*6.00*

Classical molecular dynamics simulations of $xMgO-(50-x)CaO-50SiO_2$ systems where x varies from x=0 to x=50 in steps of 5 were performed using DLPOLY 2.0 [18]. The glass densities for the end member compositions (x=0, and x=50) were obtained from the literature [19], [20]. It was assumed that the glass densities of the intermediate compositions were a linear combination of the end member densities. Each system contained 3,000 atoms within a cubic box which had a side length of approximately 33 Å. The time-step was 2fs, and the relaxation time was 2ps. An NVT Berendsen thermostat was used throughout and all simulation stages were fully equilibrated.

A random starting configuration was used and each simulation began at 5000K to ensure a homogeneous distribution of atoms. The system was then successively cooled to 2000K in steps of 100K before being quenched to 300K at a rate of $10^{13} Ks^{-1}$. The single temperature stages ran for 5,000 timesteps while the quench stage required 85,000 timesteps. A stage at 300K followed to ensure the formation of a solid glass model and ran for 80,000 timesteps. This stage at 300K was then repeated to form the sampling stage which was used for analysis. Similar methodologies have previously been shown to produce realistic models of $yMgO-(100-y)SiO_2$ [20] and $zCaO-(100-z)SiO_2$ [19] glasses, and include the endpoint compositions ($50MgO-50SiO_2$ and $50CaO-50SiO_2$) investigated in this present study.

To study dynamical properties, the mean square displacement (MSD) of atoms was analysed from molecular dynamics trajectories. This was done over 20,000 timesteps at a higher temperature of 1200K to amplify the diffusivity. The temperature of 1200K was below the melting temperatures of

both endpoint compositions (the 50MgO-50SiO$_2$ and 50CaO-50SiO$_2$ endpoint compositions have melting temperatures of 1830K and 1816K respectively).

Results

Visual representations of the glass models at 300K where x=5, x=25, and x=45 are shown in figure 2. It can be seen that the modifier ion distribution appears to be mixed in the silicate network and that there are no obvious regions of clustering or phase separation. In order to further examine the structure of the glass models, nearest neighbour distance and coordination number values were obtained.
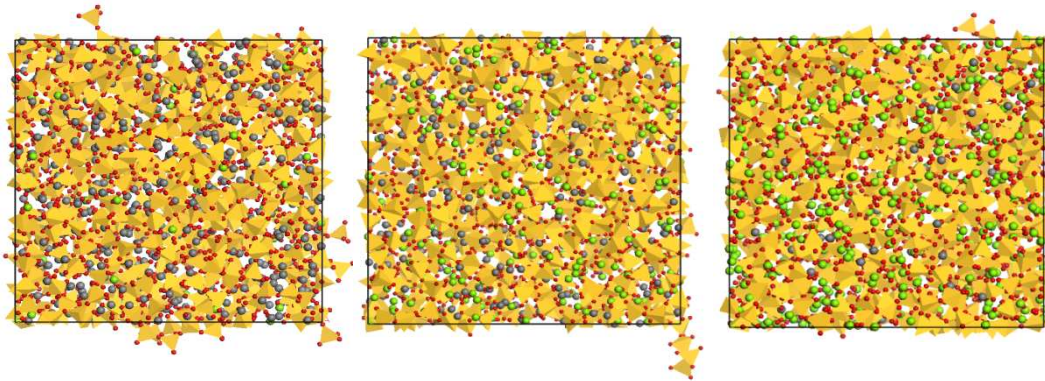

Figure 2: From left to right, glass models of xMgO-(50-x)CaO-50SiO$_2$, where x=5, x=25, and x=45. The yellow tetrahedra are silicon atoms; and the red, grey, and green spheres represent oxygen, calcium and magnesium atoms respectively.

The plots of the nearest neighbour distance as a function of x (shown in figure 3) reveal minimal variation in the nearest neighbour distance as magnesium ions are substituted for calcium ions. The short range order correlations including Si-O, O-O, and Si-Si have average nearest neighbour distances of 1.60 Å, 2.59 Å, and 3.10 Å respectively as expected for a silicate network. The average nearest neighbour distances for the remaining correlations are detailed in table 3.
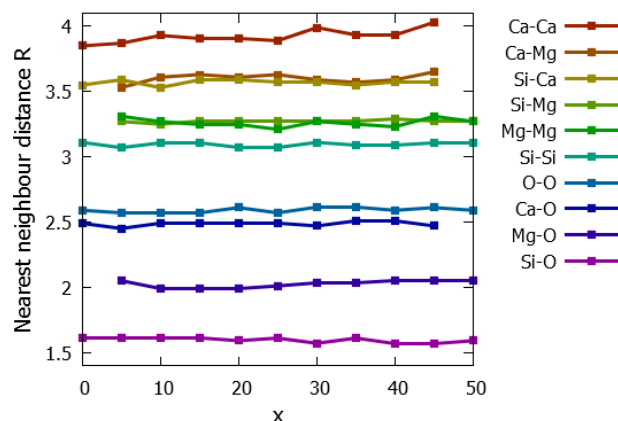

Figure 3: Nearest neighbour distances, R, as a function of x for the xMgO-(50-x)CaO-50SiO$_2$ glasses.

Table 3: Average nearest neighbour distance, R, and coordination number, N(r), values where the standard deviations have been included in the parentheses. The cut-off distances used to identify the coordination numbers are also included. Note, a '-' indicates that the values of N(r) change significantly with x.

Correlation	R	N(r)	r_{cutoff} (Å)
Si-O	1.60(2)	4.00(0)	2.00
Mg-O	2.02(3)	4.62(7)	2.75
O-O	2.59(2)	4.30(3)	2.85
Ca-O	2.49(2)	6.29(10)	3.00
Si-Si	3.10(2)	2.14(8)	3.40
Si-Mg	3.27(2)	-	3.90
Si-Ca	3.57(1)	-	4.50
Mg-Mg	3.26(5)	-	4.10
Ca-Mg	3.60(4)	-	4.70
Ca-Ca	3.92(3)	-	4.90

Coordination numbers can be obtained by integrating the pair correlation functions up to a cut-off distance r_{cutoff}. By applying the cut-off distances listed in table 3, the coordination numbers in figure 4 were attained. Figure 4 shows that the short range order (SRO) correlations such as Si-O, O-O, and Si-Si maintained almost constant coordination number values as magnesium ions were substituted for calcium ions. As quantified in table 3, the average coordination numbers of 4.0, 4.3, and 2.1 respectively were consistent with a dominant metasilicate glass network structure. The Ca-Mg, Mg-Mg, and Si-Mg coordination numbers increased linearly, while the Si-Ca and Ca-Ca coordination numbers decreased linearly as x increased.
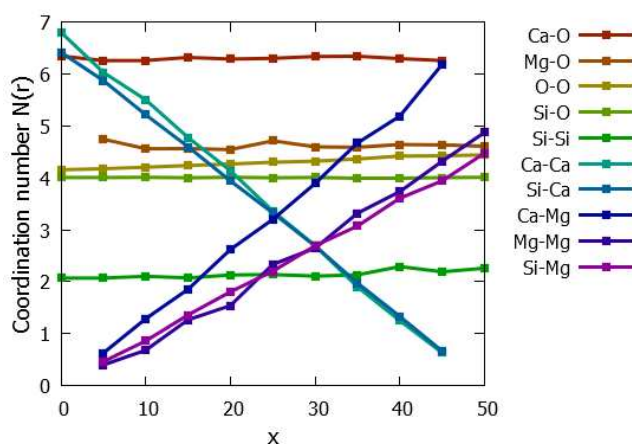

Figure 4: Coordination number values, N(r), (based on the cut-off distances in table 4) as a function of x for the xMgO-(50-x)CaO-50SiO$_2$ glasses.

The silicon network connectivity, Q^n, describes the number of bridging oxygen ions per SiO$_4$ tetrahedral structural unit, and can indicate the impact of modifier ions on the silicate network. The Q^n distributions for the glass models are shown in figure 5, where it can be seen that all of the glass models have similar Q^n distributions with the proportion of Q^2 species being dominant as expected for a metasilicate.
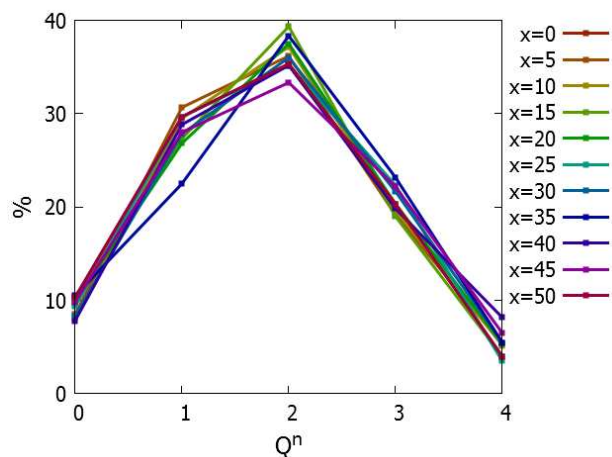
Figure 5: The silicon network connectivity, Q^n, distributions in the xMgO-(50-x)CaO-50SiO$_2$ glasses.

Mean squared displacement (MSD) measurements at 1200K were performed to investigate the dynamical properties of the glass systems. The temperature of 1200K was chosen to intensify the ion diffusion without reaching the melting temperatures of the glasses. As illustrated in figure 6, the MSD values for the oxygen and silicon ions displayed minimal variation. In contrast, there were significant deviations from linearity in the MSD values for magnesium and calcium ions, particularly when the system contained an equimolar mixture of magnesium and calcium ions. It can also be seen in figure 6 that the MSD of magnesium ions generally exceeds the MSD of calcium ions. Interestingly, there was an increase in MSD of both magnesium and calcium ions with minimal mixing, i.e. for x=5 and x=45.
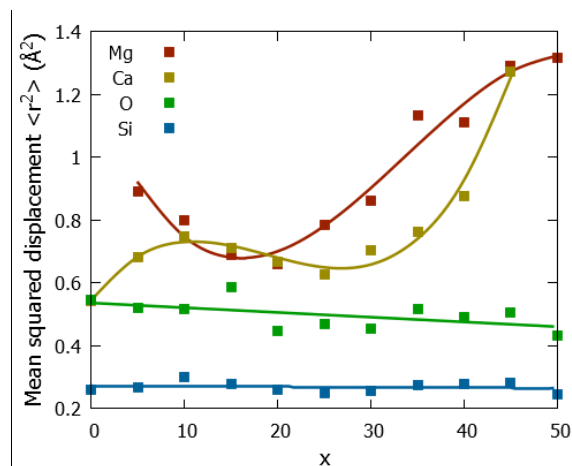

Figure 6: The mean squared displacement (MSD) values for magnesium, calcium, oxygen, and silicon ions as a function x for the xMgO-(50-x)CaO-50SiO$_2$ glasses. The magnesium and calcium ion trends have been fitted using cubic functions, whilst the oxygen and silicon ion trends were fitted using linear functions.

Discussion

The xMgO-(50-x)CaO-50SiO$_2$ system was ideally suited to investigate whether any MAEE would occur when two different types of alkaline earth ion were present in a glass system. This is partly due to the simplicity of the glass compositions which only contained silicate tetrahedra and two types of alkaline earth ions. There were no other ions in the system, such as alkaline ions, that could have

affected the above results. Additionally, the glass compositions contained a high alkaline earth content of 50% which enabled any MAEE present to be readily detected.

Figure 3 showed that the nearest neighbour distances for all correlations remained almost constant as magnesium ions were substituted for calcium ions. Similarly, the coordination numbers for all short range order correlations (figure 4) were almost constant as magnesium ions were substituted for calcium ions. The Ca-Mg, Mg-Mg, and Si-Mg coordination number values predictably rose linearly as x increased due to the increasing proportion of magnesium ions in the system. Conversely, the Mg-Ca, Ca-Ca, and Si-Ca coordination numbers decreased linearly as x increased due to the decreasing proportion of calcium ions in the system. This linear increase or decrease in coordination number was a significant result because it showed that the alkaline earth ions in the glass systems were stochastically mixed (figure 7). In addition, since deviations beyond those caused by limited statistics were not observed in figures 3 and 4, it was evident that the MAEE was not a structural effect, analogous with the conclusions drawn about the MAE [2].
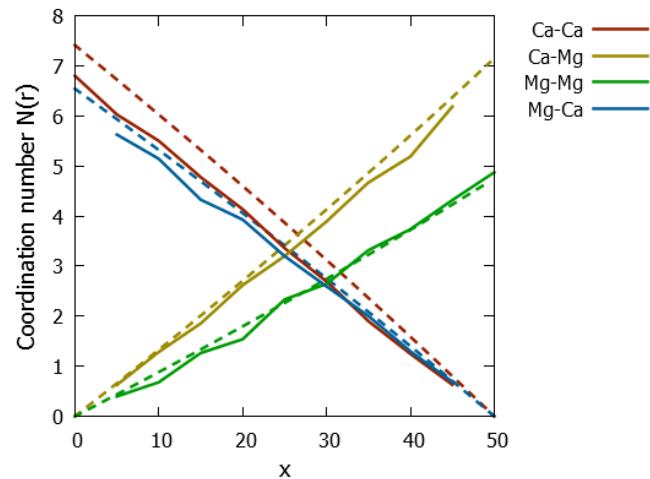

Figure 7: The coordination number, N(r), trends in the $xMgO\text{-}(50\text{-}x)CaO\text{-}50SiO_2$ glass models (solid lines) compared to the expected trends (dashed lines) based on the atomic number density and cut-off distances applied.

Since structural analyses were conducted within the immediate local environment, and alkaline earth ions were not affected by other alkaline earth ions in this vicinity, it was important to consider the atomic environment on a less local scale and begin to study the dynamics of the glasses. The mean squared displacement plot in figure 6 showed that ion diffusivity was at its highest when x was large. Figure 6 also showed that the diffusivity of calcium ions was generally lower than that of magnesium ions. This is because a calcium ion is of greater mass compared to a magnesium ion, causing it to exhibit greater inertia. Although the alkaline earth ion diffusivity was expected to increase linearly, it was clearly suppressed around x=25, providing evidence for a MAEE. Since ions are known to migrate between adjacent sites [2], and the glasses are stochastically mixed, it was evident that diffusivity was not preferred between dissimilar alkaline earth ions, hindering ion hopping analogous to the MAE [5]. The prevention of ion hopping is likely to be caused by the difference in ion site volumes between magnesium and calcium ions. Since calcium ions have a larger ionic radius compared to magnesium ions (as illustrated by the relative average Ca-O and Mg-O nearest neighbour distances of 2.49 Å and 2.02 Å respectively in figure 3), it would be difficult for a calcium ion to diffuse into a magnesium ion site. The heightened alkali earth ion diffusivity for compositions containing minimal proportions of magnesium or calcium ions (i.e. at x=5, x=45) in

figure 6 is likely to have been caused by an increase in the entropy of the system, encouraging higher diffusivity. However, this requires further investigation.

Conclusion

In conclusion, the $xMgO$-$(50-x)CaO$-$50SiO_2$ system was ideal for investigating whether a MAEE occurs in an analogous manner to the MAE. This was due to the simplicity of the compositions and the high alkaline earth ion content of 50%. Structural investigations included nearest neighbour distance, coordination number, and silicon network connectivity calculations. None of the nearest neighbour distances or coordination number values exhibited deviations beyond those caused by the limited statistics of the models. The linear increase in the Ca-Mg, Mg-Mg, and Si-Mg coordination numbers and the linear decrease in the Mg-Ca, Ca-Ca, and Si-Ca coordination numbers elucidated that the alkaline earth ions were stochastically mixed in the glasses. An absence of any significant deviation from the expected trends in the structural investigations confirmed that the MAEE is not a structural effect. By calculating mean squared displacement values at 1200K, a significant suppression in the alkaline earth ion diffusivity for an equimolar mixture of calcium and magnesium ions (around x=25) was observed. It therefore became apparent that the MAEE influences the dynamic properties of the glass and is analogous to the MAE. The MAEE is likely to be caused by differences in ionic radius and mass between the two alkaline earth ions in the system.

References

[1]   G. N. Greaves, "EXAFS and the structure of glass," *J. Non. Cryst. Solids*, vol. 71, no. 1–3, pp. 203–217, 1985.

[2]   G. N. Greaves and S. Sen, "Inorganic glasses, glass-forming liquids and amorphizing solids," *Adv. Phys.*, vol. 56, no. 1, pp. 1–166, 2007.

[3]   C. T. Moynihan, N. S. Saad, D. C. Tran, and A. V. Lesikar, "Mixed-Alkali Effect in the Dilute Foreign-Alkali Region. Failure of the Strong Electrolyte/Cationic Interaction Model," *J. Am. Ceram. Soc.*, vol. 63, no. 7–8, pp. 458–464, 1980.

[4]   J. Kjeldsen, M. M. Smedskjaer, J. C. Mauro, R. E. Youngman, L. Huang, and Y. Yue, "Mixed alkaline earth effect in sodium aluminosilicate glasses," *J. Non. Cryst. Solids*, vol. 369, pp. 61–68, 2013.

[5]   P. Maass, A. Bunde, and M. D. Ingram, "Ion-Transport Anomalies in Glasses," *Phys. Rev. Lett.*, vol. 68, no. 20, pp. 3064–3067, 1992.

[6]   R. Kirchheim, "The mixed alkali effect as a consequence of network density and site energy distribution," *J. Non. Cryst. Solids*, vol. 272, no. 2–3, pp. 85–102, 2000.

[7]   B. Roling and M. D. Ingram, "Mixed alkaline-earth effects in ion conducting glasses," *J. Non. Cryst. Solids*, vol. 265, no. 1–2, pp. 113–119, 2000.

[8]   P. Maass, "Towards a theory for the mixed alkali effect in glasses," *J. Non. Cryst. Solids*, vol. 255, no. 1, pp. 35–46, 1999.

[9]   D. Teter, "Private communication." 2004.

[10]   J. D. Gale, "GULP: A computer program for the symmetry-adapted simulation of solids," *J. Chem. Soc. Faraday Trans.*, vol. 93, no. 4, pp. 629–637, 1997.

[11]   R. F. Fletcher, D.A.; McMeeking, "The United Kingdom chemical database service," *J. Chem. Inf. Comput. Sci.*, vol. 36, no. 4, pp. 746–749, 1996.

[12]   M. A. Ghebouli, B. Ghebouli, A. Bouhemadou, M. Fatmi, and K. Bouamama, "Structural, electronic, optical and thermodynamic properties of $Sr_xCa_{1-x}O$, $Ba_xSr_{1-x}O$ and $Ba_xCa_{1-x}O$ alloys," *J. Alloys Compd.*, vol. 509, no. 5, pp. 1440–1447, 2011.

[13]   R. M. Hazen, "Effects of temperature and pressure on the cell dimension and X-ray temperature factors of periclase," *Am. Mineral.*, vol. 61, pp. 266–271, 1976.

[14]   A. N. Nikitin, G. V Markova, A. M. Balagurov, R. N. Vasin, and O. V Alekseeva, "Investigation of the structure and properties of quartz in the α-β transition range by neutron diffraction and mechanical spectroscopy," *Crystallogr. Reports*, vol. 52, no. 3, pp. 428–435, 2007.

[15]   Y. Ohashi, "Polysynthetically-twinned structures of enstatite and wollastonite," *Phys. Chem. Miner.*, vol. 10, pp. 217–229, 1984.

[16]   S. Sasaki, K. Fujino, Y. Takeuchi, and R. Sadanaga, "On the estimation of atomic charges by the X-ray method for some oxides and silicates," *Acta Crystallogr. Sect. A Cryst. Physics, Diffraction, Theor. Gen. Crystallogr.*, vol. 36, no. 6, pp. 904–915, 1980.

[17]   R. M. Thompson and R. T. Downs, "Model pyroxenes II: Structural variation as a function of tetrahedral rotation," *Am. Mineral.*, vol. 89, no. 4, pp. 614–628, 2004.

[18]   W. Smith and T. R. Forester, "DL_POLY_2. 0: A general-purpose parallel molecular dynamics simulation package," *J. Mol. Graph.*, vol. 14, no. 3, pp. 136–141, 1996.

[19]   R. N. Mead and G. Mountjoy, "A Molecular Dynamics Study of the Atomic Structure of $(CaO)_x$ $(SiO_2)_{1-x}$ Glasses," *J. Phys. Chem. B*, vol. 110, no. 29, pp. 14273–14278, 2006.

[20]   B. M. Al-Hasni and G. Mountjoy, "A molecular dynamics study of the atomic structure of x(MgO) 100–x(SiO_2)," *J. Non. Cryst. Solids*, vol. 400, pp. 33–44, 2014.

[21]   "MS Modelling version 3.2." Accelerys Software Inc., Cambridge, UK, 2005.